Photon-Assisted Charge-Parity Jumps in a Superconducting Qubit

M. Houzet,[1] K. Serniak,[2] G. Catelani,[3,4] M. H. Devoret,[2] and L. I. Glazman[2]

[1]*Univ. Grenoble Alpes, CEA, IRIG-Pheliqs, F-38000 Grenoble, France*
[2]*Departments of Physics and Applied Physics, Yale University, New Haven, Connecticut 06520, USA*
[3]*JARA Institute for Quantum Information (PGI-11), Forschungszentrum Jülich, 52425 Jülich, Germany*
[4]*Yale Quantum Institute, Yale University, New Haven, Connecticut 06520, USA*

We evaluate the rates of energy and phase relaxation of a superconducting qubit caused by stray photons with energy exceeding the threshold for breaking a Cooper pair. All channels of relaxation within this mechanism are associated with the change in the charge parity of the qubit, enabling the separation of the photon-assisted processes from other contributions to the relaxation rates. Among the signatures of the new mechanism is the same order of rates of the transitions in which a qubit loses or gains energy, which is in agreement with recent experiments. Our theory offers the possibility to characterize the electromagnetic environment of superconducting devices at the single-photon level for frequencies above the super-conducting gap.

Introduction.—The electromagnetic environment is known to affect the operation of any superconducting device based on tunnel junctions [1–3] through photon-assisted tunneling [4]. The spectral content and origin of this environment are not known *a priori*. This is why phenomenological approaches, such as the $P(E)$ theory [5], are conventionally used to model (but not explain) the environment. In this work, we give a route towards its characterization at the single-photon level. Namely, we consider the photon-induced relaxation of superconducting qubits in the circuit-QED setting [6–11]. We find that measuring it actually opens—with the help of our theory—an experimental path for acquiring information on the environment by focusing on its high-frequency component.

When a Josephson junction absorbs a photon with energy $\hbar\omega > 2\Delta$ capable of breaking a Cooper pair, a single electron is transferred across the junction (here, Δ is the BCS energy gap). If the junction is a part of a superconducting qubit, such an e jump can be detected by monitoring the charge parity of the device [12–16]. An e jump may also result in a transition to a different qubit state, and we evaluate the rates of all transitions that change charge parity. We find that the transition rates for the photon-assisted e jumps differ qualitatively from those initiated by steady-state quasiparticles residing in the electrodes [17–23]. The rates thus provide a clear fingerprint of the absorbed photon. Moreover, in the popular transmon design, a small Josephson junction is located inside a microwave cavity. Photons are brought inside the cavity through coaxial cables, and their electric field is concentrated at the junction. Therefore, a single photon turns out to be way more effective than a resident quasiparticle in causing the e jumps and, in turn, causes energy and phase-coherence relaxation associated with

them in state-of-the-art devices. Recent experiments performed with transmons have directly correlated qubit transitions with e jumps [13,15]. Our theory explains the experimental findings [15].

Photon-assisted e-jump rates.—The role of quasiparticles in an elementary superconducting qubit is captured by the electronic Hamiltonian

$$\hat{H}_{\mathrm{el}} = \hat{H}_\varphi + \hat{H}_{\mathrm{qp}} + \hat{H}_T. \qquad (1)$$

The first term here describes the quantum dynamics of the superconducting phase difference across a Josephson junction,

$$\hat{H}_\varphi = 4E_C(\hat{N} - n_g)^2 - E_J \cos\hat{\varphi} + \frac{1}{2}E_L(\hat{\varphi} - 2\pi\Phi_e/\Phi_0)^2, \qquad (2)$$

where $\hat{\varphi}$ and $\hat{N} = -id/d\hat{\varphi}$ are canonically conjugate quantum variables describing the superconducting phase difference and the number of Cooper pairs that tunneled across the junction, respectively; E_J and $4E_C$ are the Josephson and charging energies associated with these two variables; and n_g is a dimensionless gate voltage that accounts for offset charges. The inductive shunt of a fluxonium [24] is described by the last term in Eq. (2); its presence allows one to use an external magnetic flux Φ_e to tune the qubit levels (Φ_0 is the superconducting flux quantum). A transmon does not have a shunt; $E_L = 0$. Our theory is equally applicable to any device. The eigenstates of Eq. (2) are the qubit states $|n\rangle$ with energy E_n. The second term in Eq. (1) describes quasiparticles residing in the superconducting leads,

$$\hat{H}_{\mathrm{qp}} = \sum_{k\sigma} \varepsilon_k \hat{\alpha}^\dagger_{k\sigma} \hat{\alpha}_{k\sigma} + \sum_{p\sigma} \varepsilon_p \hat{\gamma}^\dagger_{p\sigma} \hat{\gamma}_{p\sigma}. \qquad (3)$$

Here, $\hat{\alpha}_{k\sigma}$ is a fermionic annihilation operator for a Bogoliubov quasiparticle in orbital state k and with spin σ in one of the leads, and $\hat{\gamma}_{p\sigma}$ plays a similar role for a quasiparticle in the other lead ($\sigma = \pm$ for up and down spins); the quasiparticle energy $\varepsilon_k = \sqrt{\xi_k^2 + \Delta^2}$ is expressed in terms of the normal-state electron energy ξ_k measured from the Fermi level. Finally, the third term in Eq. (1) describes electron tunneling across the junction,

$$\hat{H}_T = \sum_{kp\sigma} [t e^{i\hat{\varphi}/2} \hat{a}^\dagger_{k\sigma} \hat{c}_{p\sigma} + \mathrm{H.c.}] + E_J \cos \hat{\varphi}; \qquad (4)$$

it accounts for the coupling between $\hat{\varphi}$ and quasiparticle degrees of freedom. Here, the tunnel matrix element t is related to E_J through the Ambegaokar-Baratoff relation $E_J = g_T \Delta / 4$, where $g_T = 4\pi^2 \nu_0^2 |t|^2$ is the conductance of the junction in the normal state (in units of $e^2/\pi\hbar$) and ν_0 is the normal density of states per spin. The operator $\hat{a}_{k\sigma} = u_k \hat{\alpha}_{k\sigma} + \sigma v_k \hat{\alpha}^\dagger_{k\bar{\sigma}}$ (with $\bar{\sigma} = -\sigma$) annihilates an electron in one of the leads, and $u_k, v_k = \sqrt{(1 \pm \xi_k/\varepsilon_k)/2}$ are BCS coherence factors (relations for the electron annihilation operator $\hat{c}_{p\sigma}$ in the other lead are similar). The last term in Eq. (4) is included to avoid double counting the Josephson energy term appearing in Eq. (2) [19].

The coupling of the electronic degrees of freedom to an electromagnetic mode in the cavity is described by the Hamiltonian

$$\hat{H} = \hat{H}_{\mathrm{cav}} + \hat{H}_{\mathrm{el}}, \qquad \hat{H}_{\mathrm{cav}} = \hbar\omega_\nu \hat{b}^\dagger_\nu \hat{b}_\nu, \qquad (5)$$

provided that we make the substitution

$$\hat{\varphi} \to \hat{\varphi} + \phi_\nu(\hat{b}_\nu + \hat{b}^\dagger_\nu) \quad \text{with} \quad \phi_\nu = 2e\mathcal{U}_\nu/(\hbar\omega_\nu) \qquad (6)$$

in $\hat{H}_{\mathrm{el}}$. Here, $\hat{b}_\nu$ is the bosonic annihilation operator for a cavity mode ν with frequency ω_ν and an operator of the electric field $\hat{\mathcal{E}}(\mathbf{r}) = -i\mathcal{E}_\nu(\mathbf{r})(\hat{b}_\nu - \hat{b}^\dagger_\nu)$. The "zero-point fluctuation" of the phase, ϕ_ν, and voltage drop, $\mathcal{U}_\nu$, across the Josephson junction are proportional to the electric field $\mathcal{E}_\nu(\mathbf{r})$; for definiteness, we relate $\mathcal{U}_\nu$ to the field value at the junction, $\mathcal{U}_\nu = d_\nu \mathcal{E}_\nu(0)$. In general, the effective length d_ν depends not only on the specific geometry of the qubit but also on the frequency ω_ν. Inserting the substitution rule [Eq. (6)] into Eq. (4) and accounting for the weakness of coupling ($\phi_\nu \ll 1$), we express the Hamiltonian of the quasiparticle-photon-qubit interaction as

$$\delta\hat{H}_T = \frac{i\phi_\nu}{2}(\hat{b}_\nu + \hat{b}^\dagger_\nu)(\hat{V}_1 + \hat{V}_2) + \mathrm{H.c.},$$

$$\hat{V}_1 = t\sum_{kp\sigma}(e^{i\hat{\varphi}/2} u_k u_p + e^{-i\hat{\varphi}/2} v_k v_p)\hat{\alpha}^\dagger_{k\sigma}\hat{\gamma}_{p\sigma},$$

$$\hat{V}_2 = t\sum_{kp\sigma}\sigma(e^{i\hat{\varphi}/2} u_k v_p - e^{-i\hat{\varphi}/2} v_k u_p)\hat{\alpha}^\dagger_{k\sigma}\hat{\gamma}^\dagger_{p\bar{\sigma}}. \qquad (7)$$

Treating $\delta\hat{H}_T$ as a perturbation to $\hat{H}_0 = \hat{H}_\varphi + \hat{H}_{\mathrm{qp}} + \hat{H}_{\mathrm{cav}}$, and assuming a vanishing occupation of the quasiparticle states to neglect $\hat{V}_1$, we can use the Fermi's golden rule to evaluate the rate for absorbing a cavity photon while changing the qubit state from n to m,

$$\Gamma_{nm} = \frac{2\pi}{\hbar}\left(\frac{\phi_\nu}{2}\right)^2 \sum_{kp\sigma}|\langle \mathrm{vac}, m|\hat{\alpha}_{k\sigma}\hat{\gamma}_{p\bar{\sigma}}\hat{V}_2|\mathrm{vac}, n\rangle|^2$$

$$\times \delta(\hbar\omega_\nu + E_n - E_m - \varepsilon_k - \varepsilon_p), \qquad (8)$$

where $|\mathrm{vac}, n\rangle = |\mathrm{vac}\rangle \otimes |n\rangle$ is the product of the BCS ground state and the qubit state. Evaluating the sums in Eq. (8), we can express the e-jump rates [Eq. (8)] as

$$\Gamma_{nm} = \Gamma_\nu \Bigg[\left|\langle n|\cos\frac{\hat{\varphi}}{2}|m\rangle\right|^2 S_-\left(\frac{\hbar\omega_\nu + E_n - E_m}{\Delta}\right)$$

$$+ \left|\langle n|\sin\frac{\hat{\varphi}}{2}|m\rangle\right|^2 S_+\left(\frac{\hbar\omega_\nu + E_n - E_m}{\Delta}\right) \Bigg] \qquad (9)$$

with the common characteristic scale

$$\hbar\Gamma_\nu = \frac{2}{\pi}\left(\frac{2e\mathcal{U}_\nu}{\hbar\omega_\nu}\right)^2 E_J \qquad (10)$$

for the photon absorption. Quasiparticle properties are represented by the dimensionless structure factor functions having a threshold at $\hbar\omega/\Delta \equiv x = 2$,

$$S_\pm(x) = \int_1^\infty dy \int_1^\infty dy' \frac{yy' \pm 1}{\sqrt{y^2 - 1}\sqrt{y'^2 - 1}}\delta(x - y - y'); \qquad (11)$$
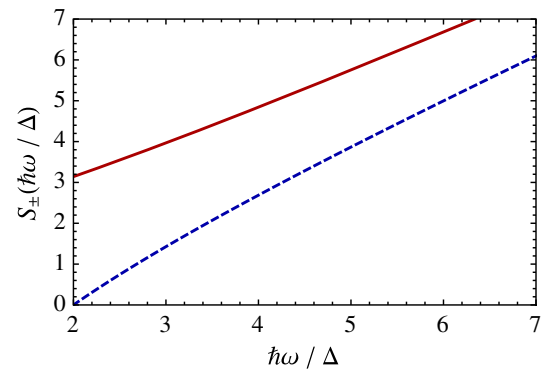

FIG. 1. Quasiparticle structure factors S_+ (solid line) and S_- (dashed line) as functions of energy at $\hbar\omega \geq 2\Delta$.

see Fig. 1. Their asymptotes are $S_-(x) = (\pi/2)(x-2)$, $S_+(x) = \pi + S_-(x)/2$ at $x - 2 \ll 2$, and $S_\pm(x) \approx x$ at $x \gg 2$. The prefactors of $S_\pm(x)$ inside the brackets of Eq. (9) are matrix elements for the transitions between qubit states. Although these matrix elements also enter into e-jump rates due to residual quasiparticles, the corresponding structure factor functions are different [23].

At $E_J \gg E_C$, Eq. (2) describes a weakly anharmonic oscillator for which the phase displays small quantum fluctuations around the classical phase φ_0. At finite E_L, it may be tuned away from zero by an external flux Φ_e and found as the solution of the equation $E_J \sin \varphi_0 + E_L(\varphi_0 - 2\pi\Phi_e/\Phi_0) = 0$, which yields the minimum of (classical) energy. In the harmonic approximation, Eq. (2) reduces to $\hat{H}'_\varphi = 4E_C(\hat{N} - n_g)^2 + \tilde{E}_J(\hat{\varphi} - \varphi_0)^2/2$ with $\tilde{E}_J = E_J \cos \varphi_0 + E_L$. The weak anharmonicity singles out the ground and excited states of the qubit. Retaining only the lowest-order correction in $(E_C/\tilde{E}_J)^{1/2}$, one obtains $\hbar\omega_{01} \approx \sqrt{8\tilde{E}_J E_C} - E_C$ for the corresponding transition frequency. Evaluation of the qubit matrix elements in Eq. (9) within the leading order [25] in $(E_C/\tilde{E}_J)^{1/2}$ yields

$$\Gamma_{00} = \Gamma_{11} = \Gamma_\nu \left[\frac{1 + \cos\varphi_0}{2} S_-\left(\frac{\hbar\omega_\nu}{\Delta}\right) + \frac{1 - \cos\varphi_0}{2} S_+\left(\frac{\hbar\omega_\nu}{\Delta}\right) \right], \tag{12a}$$

$$\Gamma_{01} = \Gamma_\nu \sqrt{\frac{E_C}{8\tilde{E}_J}} \left[\frac{1 + \cos\varphi_0}{2} S_+\left(\frac{\hbar\omega_\nu - \hbar\omega_{01}}{\Delta}\right) + \frac{1 - \cos\varphi_0}{2} S_-\left(\frac{\hbar\omega_\nu - \hbar\omega_{01}}{\Delta}\right) \right], \tag{12b}$$

$$\Gamma_{10} = \Gamma_\nu \sqrt{\frac{E_C}{8\tilde{E}_J}} \left[\frac{1 + \cos\varphi_0}{2} S_+\left(\frac{\hbar\omega_\nu + \hbar\omega_{01}}{\Delta}\right) + \frac{1 - \cos\varphi_0}{2} S_-\left(\frac{\hbar\omega_\nu + \hbar\omega_{01}}{\Delta}\right) \right]. \tag{12c}$$

The φ_0 dependence of the rates in Eq. (12) reveals the interference between quasiparticles crossing the junction in the photon-absorption process. It is reminiscent of the $\cos\varphi$ effect in the dissipative Josephson current [26] and flux-dependent fluxonium relaxation rates [27]. At $E_L \neq 0$, ω_{01} is independent of n_g, which can be gauged out from H'_φ. Sensitivity of the qubit energy levels to the gate voltage is useful for separating out the rates of various e-jump processes [13,15]. The φ_0 dependence of the rates in Eq. (12) may be investigated in a device retaining such sensitivity, e.g., in a flux qubit [14,28].

Let us make several observations. First, at a large frequency $\hbar\omega_\nu \gg 2\Delta$, the transition rates are independent of φ_0, and we find $\Gamma_{01}/\Gamma_{10} \approx 1$ and

$$\Gamma_{00}/\Gamma_{10} = (8\tilde{E}_J/E_C)^{1/2}. \tag{13}$$

Notably, rates Γ_{00} and Γ_{11}, in which a qubit state does not change, are substantially larger than Γ_{01} and Γ_{10}. Furthermore, at $\varphi_0 = 0$ and $\hbar\omega_{01} \ll \Delta$, we find

$$1 - \hbar\omega_{01}/\Delta < \Gamma_{01}/\Gamma_{10} < 1 \tag{14}$$

at any frequency above the threshold: $\hbar\omega_\nu > 2\Delta + \hbar\omega_{01}$. Finally, at $\hbar\omega_\nu$ close to the threshold, the large factor in Eq. (13) is compensated for by a small factor from $S_-(x)$, resulting in

$$\frac{\Gamma_{00}}{\Gamma_{10}} \approx \left(\frac{2\tilde{E}_J}{E_C}\right)^{1/2}\left(\frac{\hbar\omega_\nu}{\Delta} - 2\right) \quad \text{at } \hbar\omega_\nu - 2\Delta \ll \Delta. \tag{15}$$

The characteristic rate Γ_ν of Eq. (10) depends on the qubit parameter d_ν and the amplitude of the quantized electric field $\mathcal{E}_\nu$. To estimate the two, we notice that, in conventional 3D designs [8], the superconducting circuit is oriented along the shortest direction of a 3D electromagnetic cavity: say, with a width L_z along the z direction much smaller than the characteristic transverse sizes: L_x, $L_y \gg L_z$. Therefore, the electric field at frequencies smaller than $\pi c/L_z$ (c is the light velocity) is expressed in terms of the TE modes,

$$\hat{\mathcal{E}} = -i\sum_\nu (\hat{b}_\nu - \hat{b}_\nu^\dagger)\mathcal{E}_\nu(x, y)\hat{z}, \tag{16}$$

and is independent of z, apart from the vicinity of the qubit and rf input or output connectors constituting perturbing metallic boundary conditions inside the cavity. Furthermore, $\mathcal{E}_\nu(x, y)$ is a real solution of the equation

$$[\omega_\nu^2 + c^2(\partial_x^2 + \partial_y^2)]\mathcal{E}_\nu(x, y) = 0 \tag{17}$$

at frequency ω_ν in the transverse (x, y) plane, which is complemented with the appropriate nonradiative boundary conditions defined by the cavity walls and the above-mentioned perturbations in the cavity. Because the perturbations occupy a tiny fraction of the cavity volume, we may disregard them in the normalization condition to obtain

$$\overline{\mathcal{E}_\nu^2} = 2\pi\hbar\omega_\nu/(AL_z). \tag{18}$$

Here, $\overline{\mathcal{E}_\nu^2} = (1/A) \int d^2r \mathcal{E}_\nu^2(x, y)$, and A is the cavity's transverse area.

Given the presence of perturbations, we expect that the boundary conditions associated with Eq. (17) will yield a chaotic behavior for its solutions [29]. The spacing of eigenfrequencies around a given frequency ω_ν is estimated as $\delta\omega = c^2/(A\omega_\nu)$. Then, the amplitude of the electric field at the qubit position will fluctuate from mode to mode. We may use the random matrix theory (RMT) [30] to describe these fluctuations in a range of frequencies of the order $c/\sqrt{A}$ around a frequency ω_ν such that $c/\sqrt{A} \ll \omega_\nu \lesssim \pi c/L_z$, where $\pi c/L_z$ is the cutoff frequency for the TM modes. Therefore, the amplitude of the electric field at a given position is given by the Porter-Thomas distribution in the orthogonal ensemble,

$$P(\mathcal{E}_\nu^2)d\mathcal{E}_\nu^2 = (2\pi\mathcal{E}_\nu^2\langle\mathcal{E}_\nu^2\rangle)^{-1/2} \exp(-\mathcal{E}_\nu^2/2\langle\mathcal{E}_\nu^2\rangle)d\mathcal{E}_\nu^2, \tag{19}$$

where the brackets denote the ensemble average. For the modes ν that can be described with the RMT, the spatial and ensemble averages equal each other: $\langle\mathcal{E}_\nu^2\rangle = \overline{\mathcal{E}_\nu^2}$.

The effective length d_ν, which characterizes the coupling between the superconducting circuit and the electric field, is frequency independent in a wide frequency range. This range is limited by the requirement that the size of the superconducting circuit is smaller than the wavelength of the photon $\lambda_\nu = 2\pi c/\omega_\nu$, whereas the inductance $L_J = \hbar^2/(4e^2E_J)$ of the Josephson junction is high enough to treat it as an open circuit: $L_J\omega_\nu \gg Z_{\text{vac}}$ (here, Z_{vac} is the vacuum impedance). For a typical design, the frequency of stray photons with $\hbar\omega \sim 2\Delta$ falls below the upper limit set by the former condition; the much lower transition frequency ω_{01} exceeds the lower limit set by the latter condition, as long as $\sqrt{E_C/\tilde{E}_J} \gg \alpha$ (here, $\alpha = e^2/\hbar c$ is the fine structure constant). We may extract the frequency-independent $d_\nu \equiv d$ from the dispersive shift measured at the resonator's principal mode frequency ω_r, which is close to ω_{01}. Indeed, ignoring the role of quasiparticles and projecting the Hamiltonian (5) onto the lower-energy states of the qubit yields

$$\hat{H} = \hbar\omega_r\hat{b}_r^\dagger\hat{b}_r + \frac{\hbar\omega_{01}}{2}\sigma_z + \hbar g(\hat{b}_r + \hat{b}_r^\dagger)\sigma_x, \tag{20}$$

where

$$g = \frac{1}{\hbar}(2E_C\tilde{E}_J^3)^{1/4}\frac{2ed\mathcal{E}_r}{\hbar\omega_r} \tag{21}$$

is the "vacuum Rabi frequency" [31], and σ_x and σ_z are Pauli matrices acting in the two-dimensional space of qubit states. Combining Eqs. (10), (18), and (21) then yields

$$\Gamma_\nu = \frac{4}{\pi}\frac{g^2}{\omega_{01}}\frac{\omega_r}{\omega_\nu}\frac{E_J}{\tilde{E}_J}\left(\frac{\mathcal{E}_r^2(x, y)}{\bar{\mathcal{E}}_r^2}\right)^{-1}\frac{\mathcal{E}_\nu^2(x, y)}{\bar{\mathcal{E}}_\nu^2}, \tag{22}$$

where (x, y) is the vicinity of the qubit location. Using the standard expression for the principal mode in a rectangular cavity, and assuming that the qubit is positioned near the cavity's center, allows us to estimate $\mathcal{E}_r^2(x, y)/\bar{\mathcal{E}}_r^2 \approx 4$. The ensemble-averaged value of Eq. (22) is then

$$\langle\Gamma_\nu\rangle = \frac{\Delta}{\hbar\omega_\nu}\Gamma_0, \qquad \Gamma_0 = \frac{1}{\pi}\frac{g^2}{\omega_{01}}\frac{\hbar\omega_r}{\Delta}\frac{E_J}{\tilde{E}_J}. \tag{23}$$

In the two-level approximation for the qubit states, g is related to the dispersive shift of the qubit transition frequency: $\chi = g^2/|\omega_r - \omega_{01}|$. Equations (12) and (23) express the main result of this work.

e jumps in transmons.—From now on, we specify the discussion to transmons, such that $\tilde{E}_J = E_J$ and $\varphi_0 = 0$. There are two aspects in which the rates of charge-parity transitions caused by photons differ qualitatively from those caused by the quasiparticles resident in the qubit. First, it is the approximately equal rates of transitions accompanied by the qubit energy loss or gain: $\Gamma_{01} \approx \Gamma_{10}$; see Eq. (14). To the contrary, the resident quasiparticles mechanism [23] leads to $\Gamma_{01} \ll \Gamma_{10}$, even if their energy distribution is out of equilibrium [32]. Second, the ratio Γ_{00}/Γ_{10} is large; see Eq. (13). In contrast, the quasiparticle tunneling mechanism yields a parametrically smaller result [23], differing from Eq. (13) by an additional factor of $(\hbar\omega_{01}T_{\text{qp}}/\pi\Delta^2)^{1/2} \ll 1$; here, $T_{\text{qp}} \ll \Delta$ is the effective temperature of the quasiparticles.

A single photon with energy $\hbar\omega > 2\Delta$ is much more effective in causing decoherence than the residual quasiparticle density in a typical setting. This efficiency is a byproduct of the efficient coupling between the superconducting circuit and the electromagnetic cavity in the transmon design. The quasiparticle mechanism [17] yields $\Gamma_{10}^{\text{qp}} = x_{\text{qp}}\sqrt{2\Delta\omega_{01}/\pi^2\hbar}$, where $x_{\text{qp}} = n_{\text{qp}}/(2\nu_0\Delta)$ is the quasiparticle density in units of the density of Cooper pairs. We compare the effectiveness of a single photon with that of quasiparticles by equating $\langle\Gamma_{10}\rangle = \Gamma_{10}^{\text{qp}}$ and finding the corresponding $x_{\text{qp}}^{\text{eff}}$,

$$x_{\text{qp}}^{\text{eff}} = \sqrt{2}\pi^2\alpha\sqrt{\frac{\hbar\omega_{01}}{\Delta}}\frac{d^2\lambda_\nu}{AL_z}. \tag{24}$$

For a typical device [31], this yields $x_{\text{qp}}^{\text{eff}} \sim 5 \times 10^{-5}$ much larger than the typical residual density [8] of $\lesssim 10^{-6}$.

Comparison with experiment.—Photon-assisted *e* jumps provide a natural explanation for the results of the recent experiment [15]. In [15], the rates of the *e* jumps accompanied by qubit excitation and relaxation, respectively, were approximately equal each other. This observation is

consistent with Eq. (14) and hints at a finite probability n_ν of finding a high-energy photon in the cavity. Furthermore, we may associate the observed rate of e jumps occurring without the qubit leaving the ground state with the rate of $n_\nu \Gamma_{00}$, whereas the above-mentioned measured rate of $1 \rightarrow 0$ transitions is associated with $n_\nu \Gamma_{10}$, cf. Eqs. (12a) and (12c) with $\varphi_0 = 0$. Comparing the ratio of the two with the experimental data, we obtain the relation $\Gamma_{00}/\Gamma_{10} \approx 4.1$, which we treat as an equation for finding the characteristic photon frequency. Using the qubit parameters [31], we find $\omega_\nu \approx 2.8\Delta/\hbar$. Then, inserting this frequency into the ratio of rates (12b) and (12c) yields $\Gamma_{01}/\Gamma_{10} \approx 0.97$, which is close to the observed ratio between the qubit relaxation and excitation rates (accompanied by e jumps).

To assess the individual rates (rather than their ratios), we assume the incoming photons belong to a narrow (compared to ω_ν) bandwidth around the frequency ω_ν. We also assume this bandwidth is wide as compared to the mean-frequency spacing $\delta\omega$, which allows us to substitute Γ_ν in Eq. (12) by its ensemble-averaged value, cf. Eq. (23). [In the opposite case of a narrow frequency bandwidth $\ll \delta\omega$, all rates in Eq. (12) would fluctuate from mode to mode according to the Porter-Thomas distribution, cf. Eq. (19); we note also that frequencies $\hbar\omega_\nu \sim 2\Delta$ for the device parameters [31] are at the margin of validity of the condition $\omega_\nu \lesssim \pi c/L_z$ used to retain TE modes only in Eq. (16).] Inserting the device parameters [31] into Eq. (23), we find $\Gamma_0^{-1} \approx 0.6 \ \mu$s. The measured e-jump rates are much lower. This indicates that the measured rates are actually controlled by the probability for a photon to enter the cavity. The sum of all measured e-jump rates then yields the rate with which photons appear in the cavity: $dn_\nu/dt = 1/T_P$ with $T_P = 77 \ \mu$s [15]. Using this value, qubit-state probabilities $P_0 \approx P_1 \approx 1/2$, and the estimated Γ_0 in equation

$$dn_\nu/dt = n_\nu \sum_{n,m=0,1} P_n \langle \Gamma_{nm} \rangle, \qquad (25)$$

we find the photon occupation factor $n_\nu \approx 10^{-2}$.

Alternatively, we may consider e jumps caused by a distribution of photons coming into the cavity from an outside thermal bath (instead of photons within a narrow frequency band). In this case, the magnitude of the e-jump rates depends on the coupling parameters between the cavity modes and the outside bath, which may depend on the frequency of incoming photons. Neglecting such dependence, the poorly known coupling parameter cancels out in the ratios between rates. In the following estimates, we consider the effect of external irradiation from a thermal bath at temperature T_b. Convolving the frequency-resolved rates (12) with the Bose-Einstein distribution and the density of modes, and assuming $\hbar\omega_{01}, T_b \ll 2\Delta$, we find

$$\Gamma_{00}/\Gamma_{10} \approx \sqrt{\frac{2E_J}{E_C}} \frac{T_b}{\Delta} \exp(-\hbar\omega_{01}/T_b), \qquad (26a)$$

$$\Gamma_{01}/\Gamma_{10} \approx \exp(-2\hbar\omega_{01}/T_b). \qquad (26b)$$

Let us note a poor agreement of the data [15] with such a uniformly attenuated thermal photons model. Indeed, equating Eq. (26a) with the corresponding observed ratio together with device parameters [31] yields $T_b \approx 0.68\Delta$. Inserting this temperature into Eq. (26b) then yields a ratio of $\Gamma_{01}/\Gamma_{10} \approx 0.77$, which is about 30% lower than the observed one. Therefore, we favor the first explanation involving photons in a relatively narrow frequency band.

Conclusion.—We have identified a decoherence channel associated with an event of photon-assisted electron tunneling through a Josephson junction in a superconducting qubit. This process results from the breaking of a Cooper pair by a stray photon with energy exceeding 2Δ and with an electric field that is concentrated at a high-impedance junction. The qubit transition rates accompanying these photon-assisted e jumps are markedly different from those caused by residual quasiparticles. They are consistent with the measured rates in Ref. [15], where charge-parity switches were equally likely to excite or relax the transmon. Interestingly, we find that the contribution per high-frequency photon in the cavity to qubit decoherence (through energy relaxation) is similar to that of low-frequency photons (through shot-noise dephasing [33]). However, this similarity depends on the particulars of the present implementation of the qubit-cavity system. Unsurprisingly, our results reinforce the importance of protecting superconducting qubits from electromagnetic radiation at all frequencies. Additionally, the control of processes unveiled in this Letter may open a perspective for the design of single-photon microwave detectors for frequencies above the gap.

---

[1] J. M. Hergenrother, J. G. Lu, M. T. Tuominen, D. C. Ralph, and M. Tinkham, Phys. Rev. B **51**, 9407 (1995).

[2] R. Deblock, E. Onac, L. Gurevich, and L. P. Kouwenhoven, Science **301**, 203 (2003).

[3] J. P. Pekola, V. F. Maisi, S. Kafanov, N. Chekurov, A. Kemppinen, Y. A. Pashkin, O.-P. Saira, M. Möttönen, and J. S. Tsai, Phys. Rev. Lett. **105**, 026803 (2010).

[4] P. K. Tien and J. P. Gordon, Phys. Rev. **129**, 647 (1963).

[5] G.-L. Ingold and Y. V. Nazarov, in *Single Charge Tunneling*, edited by H. Grabert and M. H. Devoret (Plenum, New York, 1992).

[6] A. Blais, R. S. Huang, A. Wallraff, S. M. Girvin, and R. J. Schoelkopf, Phys. Rev. A **69**, 062320 (2004).

[7] J. Koch, T. M. Yu, J. Gambetta, A. A. Houck, D. I. Schuster, J. Majer, Alexandre Blais, M. H. Devoret, S. M. Girvin, and R. J. Schoelkopf, Phys. Rev. A **76**, 042319 (2007).

[8] H. Paik, D. I. Schuster, L. S. Bishop, G. Kirchmair, G. Catelani, A. P. Sears, B. R. Johnson, M. J. Reagor, L. Frunzio, L. I. Glazman, S. M. Girvin, M. H. Devoret, and R. J. Schoelkopf, Phys. Rev. Lett. **107**, 240501 (2011).

[9] M. H. Devoret and R. J. Schoelkopf, Science **339**, 1169 (2013).

[10] S. M. Girvin, in *Quantum Machines: Measurement and Control of Engineered Quantum Systems* (Oxford University, Oxford, England, 2014).

[11] X. Gu, A. F. Kockum, A. Miranowicz, Y. X. Liu, and F. Nori, Phys. Rep. **718–719**, 1 (2017).

[12] L. Sun, L. DiCarlo, M. D. Reed, G. Catelani, Lev S. Bishop, D. I. Schuster, B. R. Johnson, Ge A. Yang, L. Frunzio, L. Glazman, M. H. Devoret, and R. J. Schoelkopf, Phys. Rev. Lett. **108**, 230509 (2012).

[13] D. Ristè, C. C. Bultink, M. J. Tiggelman, R. N. Schouten, K. W. Lehnert, and L. DiCarlo, Nat. Commun. **4**, 1913 (2013).

[14] M. Bal, M. H. Ansari, J.-L. Orgiazzi, R. M. Lutchyn, and A. Lupascu, Phys. Rev. B **91**, 195434 (2015).

[15] K. Serniak, M. Hays, G. de Lange, S. Diamond, S. Shankar, L. D. Burkhart, L. Frunzio, M. Houzet, and M. H. Devoret, Phys. Rev. Lett. **121**, 157701 (2018).

[16] K. Serniak, S. Diamond, M. Hays, V. Fatemi, S. Shankar, L. Frunzio, R. J. Schoelkopf, and M. H. Devoret, Phys. Rev. Applied **12**, 014052 (2019).

[17] J. M. Martinis, M. Ansmann, and J. Aumentado, Phys. Rev. Lett. **103**, 097002 (2009).

[18] G. Catelani, J. Koch, L. Frunzio, R. J. Schoelkopf, M. H. Devoret, and L. I. Glazman, Phys. Rev. Lett. **106**, 077002 (2011).

[19] G. Catelani, R. J. Schoelkopf, M. H. Devoret, and L. I. Glazman, Phys. Rev. B **84**, 064517 (2011).

[20] M. Lenander, H. Wang, R. C. Bialczak, E. Lucero, M. Mariantoni, M. Neeley, A. D. O'Connell, D. Sank, M. Weides, J. Wenner, T. Yamamoto, Y. Yin, J. Zhao, A. N. Cleland, and J. M. Martinis, Phys. Rev. B **84**, 024501 (2011).

[21] G. Catelani, S. E. Nigg, S. M. Girvin, R. J. Schoelkopf, and L. I. Glazman, Phys. Rev. B **86**, 184514 (2012).

[22] S. Gustavsson, F. Yan, G. Catelani, J. Bylander, A. Kamal, J. Birenbaum, D. Hover, D. Rosenberg, G. Samach, A. P. Sears, S. J. Weber, J. L. Yoder, J. Clarke, A. J. Kerman, F. Yoshihara, Y. Nakamura, T. P. Orlando, and W. D. Oliver, Science **354**, 1573 (2016).

[23] G. Catelani, Phys. Rev. B **89**, 094522 (2014).

[24] V. E. Manucharyan, J. Koch, L. I. Glazman, and M. H. Devoret, Science **326**, 113 (2009).

[25] See Ref. [23] for the next-order corrections in $(E_C/\tilde{E}_J)^{1/2}$.

[26] A. Barone and G. Paternò, *Physics and Applications of the Josephson Effect* (Wiley, New York, 2005).

[27] I. M. Pop, K. Geerlings, G. Catelani, R. J. Schoelkopf, L. I. Glazman, and M. H. Devoret, Nature (London) **508**, 369 (2014).

[28] F. Yan, S. Gustavsson, A. Kamal, J. Birenbaum, A. P. Sears, D. Hover, D. Rosenberg, G. Samach, T. J. Gudmundsen, J. L. Yoder, T. P. Orlando, J. Clarke, A. J. Kerman, and W. D. Oliver, Nat. Commun. **7**, 12964 (2016).

[29] T. Shigehara, H. Mizoguchi, T. Mishima, and T. Cheon, IEICE Trans. Fundam. Electron. Commun. Comput. Sci. **E81A**, 1762 (1998).

[30] C. W. J. Beenakker, in *The Oxford Handbook of Random Matrix Theory*, edited by G. Akemann, J. Baik, and P. Di Francesco (Oxford University, Oxford, England, 2011).

[31] Inverting Eq. (21) yields the effective length

$$d = \frac{1}{2^{5/4}\sqrt{\pi\alpha}} \frac{g}{\omega_{01}} \left(\frac{E_C}{E_J}\right)^{1/4} \sqrt{\frac{AL_z\omega_r}{c}}. \qquad (27)$$

Using the parameters of [15] ($\omega_{01}/2\pi = 4.4$ GHz, $\chi/2\pi = 3.8$ MHz, $\omega_r/2\pi = 9.2$ GHz, $E_J/E_C = 23$, $L_z = 5$ mm, and $A = 35 \times 17$ mm^2), we find $d = 1.0$ mm. With these parameters, we find $\phi_r \approx 0.03$, which is consistent with the weak-coupling assumption used to derive Eq. (7). Furthermore, $\lambda_\nu = 3$ mm for $\omega_\nu = 2\Delta/\hbar = 2\pi \times 99.4$ GHz.

[32] G. Catelani and D. M. Basko, SciPost Phys. **6**, 013 (2019).

[33] A. P. Sears, A. Petrenko, G. Catelani, L. Sun, Hanhee Paik, G. Kirchmair, L. Frunzio, L. I. Glazman, S. M. Girvin, and R. J. Schoelkopf, Phys. Rev. B **86**, 180504(R) (2012).